The potential of hydrogen-battery storage systems for a sustainable renewable-based electrification of remote islands in Norway

Journal of Energy Storage 75 (2024) 109482

Contents lists available at ScienceDirect

Journal of Energy Storage

journal homepage: www.elsevier.com/locate/est

Research Papers

The potential of hydrogen-battery storage systems for a sustainable renewable-based electrification of remote islands in Norway

Davide Trapani [a,*], Paolo Marocco [a], Domenico Ferrero [a], Karen Byskov Lindberg [b,c], Kyrre Sundseth [d], Massimo Santarelli [a]

[a] Department of Energy, Politecnico di Torino, Torino, Italy
[b] Architectural Engineering, SINTEF Community, Oslo, Norway
[c] Aneo, Trondheim, Norway
[d] New Energy Solutions Department, SINTEF Industry, Trondheim, Norway

ARTICLE INFO

Keywords:
Off-grid
Renewable energy
Hydrogen
Energy storage
Electrolysis
Remote islands

ABSTRACT

Remote locations and off-grid regions still rely mainly on diesel generators, despite the high operating costs and greenhouse gas emissions. The exploitation of local renewable energy sources (RES) in combination with energy storage technologies can be a promising solution for the sustainable electrification of these areas. The aim of this work is to investigate the potential for decarbonizing remote islands in Norway by installing RES-based energy systems with hydrogen-battery storage. A national scale assessment is presented: first, Norwegian islands are characterized and classified according to geographical location, number of inhabitants, key services and current electrification system. Then, 138 suitable installation sites are pinpointed through a multiple-step sorting procedure, and finally 10 reference islands are identified as representative case studies. A site-specific methodology is applied to estimate the electrical load profiles of all the selected reference islands. An optimization framework is then developed to determine the optimal system configuration that minimizes the levelized cost of electricity (LCOE) while ensuring a reliable 100% renewable power supply. The LCOE of the RES-based energy systems range from 0.21 to 0.63 €/kWh and a clear linear correlation with the wind farm capacity factor is observed (R^2 equal to 0.87). Hydrogen is found to be crucial to prevent the oversizing of the RES generators and batteries and ensure long-term storage capacity. The techno-economic feasibility of alternative electrification strategies is also investigated: the use of diesel generators is not economically viable (0.87–1.04 €/kWh), while the profitability of submarine cable connections is highly dependent on the cable length and the annual electricity consumption (0.14–1.47 €/kWh). Overall, the cost-effectiveness of RES-based energy systems for off-grid locations in Northern Europe can be easily assessed using the correlations derived in this analysis.

1. Introduction

The energy transition to low-carbon systems is a key challenge for the coming decades. Renewable energy sources (RES), such as wind and solar power, can play a crucial role in tackling climate change and reducing CO_2 emissions. However, the fluctuating nature and limited predictability of these energy sources, and the resulting non-dispatchability of power generation, pose several technical barriers to achieving greater RES penetration. Therefore, in order to ensure the load-supply balance while fully exploiting the RES potential, electrical energy storage (EES) solutions must be deployed. Different EES strategies can be implemented depending on the required storage capacity and duration [1]. Currently, battery storage is a mature and modular technology [2]: it is suitable for both grid-connected and stand-alone systems, but there are still some hurdles to overcome (e.g., high capital cost, limited lifetime and environmental impacts during manufacturing and disposal [1,3]), which prevent it from being feasible and cost-competitive for large-scale systems and long-term storage applications [4,5]. On the other hand, hydrogen can provide larger storage capacity and duration (without self-discharge), longer system lifetime and higher temperature tolerance, which is crucial in more extreme climates [6].

RES-based systems coupled with energy storage technologies can represent a cost-effective and sustainable strategy for the electrification

* Corresponding author.
E-mail address: davide.trapani@polito.it (D. Trapani).

https://doi.org/10.1016/j.est.2023.109482
Received 19 July 2023; Received in revised form 4 October 2023; Accepted 25 October 2023
Available online 18 November 2023

of remote areas and off-grid regions. Currently, these locations rely mainly on diesel generators (DGs), but this solution has techno-economic and environmental limitations. First, the community is exposed to fuel price fluctuations and the operating costs for fuel transportation can be very high due to the remoteness of the site [7]. Diesel generators often work at partial loads to cover the electrical demand, resulting in lower DG performance, higher fuel consumption and pollutant emissions [3]. In addition, the diesel generators require frequent maintenance and replacement of spare parts, with consequent operational downtime. Submarine cables and expansion of the national power grid, when feasible, are also being considered as alternatives to the use of diesel generators. However, the infrastructure required for the connection to the power grid can be very expensive, technically challenging and environmentally impacting [8].

Conversely, the combination of local RES and electrical energy storage can provide a clean, reliable and cost-competitive power supply that replaces diesel generators and avoids the installation of costly power transmission infrastructure. On a global scale, the potential of RES-storage systems on islands, in rural areas, desert communities and remote mountainous regions is huge. For island regions specifically, IRENA estimates that 750 million people worldwide live on more than 10,000 islands that are currently powered by 12 GW of diesel generators [9].

The increasing interest in RES-storage systems and the growing awareness of their potential in off-grid applications are confirmed by the large number of literature studies conducted in recent years [10]. Concerning battery applications, Chmiel and Bhattacharyya [11] and Gan et al. [12] evaluated the techno-economic feasibility of RES-battery systems in two Scottish sites, Isle of Eigg and Bishopton. In both cases, the RES-based solution with battery storage and backup diesel generators proved to be reliable and cost-effective: the combined use of various RES together with batteries enabled a dramatic reduction in diesel consumption while ensuring a continuous power supply. Similar results were also derived by Roy [13] for the island of Ghoramara (India), in which the PV-wind-battery-diesel configuration (with 87.8% RES penetration) turned out to be the most favourable solution. Kaldellis and Zafirakis [14] investigated the potential of hybrid PV-wind-battery systems on different islands in Greece and confirmed the advantages of using different RES simultaneously. Indeed, they found that the PV-wind system leads to a significant reduction in battery capacity, leading to a decrease in investment and operating costs. Ma et al. [15] conducted a detailed techno-economic evaluation of a PV-wind plant combined with battery storage on a small island in Hong Kong. They demonstrated the feasibility of a 100% RES-based power system and pointed out that the battery cost accounted for almost half of the total net present cost (NPC). Finally, Qi et al. [16] reported that installing a PV-battery-diesel system in the island of Quingdao (China) can reduce the cost of electricity by 27.8% compared to the fossil-based scenario.

Regarding hydrogen applications, the potential of wind-hydrogen plants was investigated in the off-grid Arctic communities of Grimsey (Iceland) [8] and Mykines (Faroe Islands) [17]. In both studies, the long-term hydrogen storage capacity was found to be necessary to improve the exploitation of wind power and to address the variability and seasonality of load and renewable production. The effectiveness of high-capacity hydrogen storage has also been confirmed in completely different climates and latitudes. Kalinci et al. [4] performed a techno-economic analysis of a stand-alone renewable energy system in the island of Bozcada (Turkey) and showed that hydrogen is required to compensate for the monthly variations in solar radiation and wind speed. In addition, Parissis et al. [18] and Tzamalis et al. [19] analyzed the role of hydrogen in the sustainable electrification of the islands of Corvo (Portugal) and Milos (Greece), showing that the use of hydrogen can significantly reduce fossil fuel demand and greenhouse gas emissions. Similar considerations were derived by Fragoso et al. [20] for the island of Flores (Portugal), in which the diesel consumption can be reduced by 76% when hydrogen is adopted to store excess wind power production.

Several studies have shown the profitability of installing hybrid storage solutions. Marocco et al. [21] and Dong et al. [22] compared the levelized cost of electricity (LCOE) of different energy system configurations for the island of Ginostra (Italy) and Zhejiang (China), respectively. Their results demonstrated that the hydrogen-battery storage is more cost-effective than the only-hydrogen and only-battery architectures. Zhang et al. [23] confirmed that the adoption of hybrid storage system in the island of Ui (South Korea) leads to a lower LCOE compared to the only-battery configuration and significantly reduces the installed battery capacity (−52%). Storage hybridization proved to be the cheapest solution also in the island of Pantelleria (Italy) and a 60% reduction in NPC was reported compared to the only-battery alternative [24]. Moreover, Groppi et al. [25] investigated the integration of battery and hydrogen storage systems in the island of Favignana (Italy) and highlighted that hybrid storage is the most viable option when local transport is included in the analysis. Finally, Tariq [26] suggested that the energy storage hybridization enables higher RES penetration in large-scale systems, such as on the island of Bonaire (Caribbean Netherlands).

The present work has been developed in the framework of the European project REMOTE, whose aim is to demonstrate the techno-economic feasibility of hydrogen-battery power-to-power (P2P) systems in different isolated areas in Europe [27]. The main objective of this study is to evaluate the potential for the installation of renewable P2P systems in remote islands in Norway. Based on the promising results of the REMOTE Norwegian case study [28,29], the replicability of these RES-based energy systems throughout the Country deserves to be carefully investigated. No studies of renewable P2P systems on Norwegian islands were found, with the exception of [30], which evaluated the performance of the Utsira pilot plant. Moreover, to the authors' knowledge, the national-scale assessment represents a novelty: while most of the literature focuses on a single case study, this article provides a comprehensive analysis of 10 reference islands (representative of 138 Norwegian island sites) and derives correlations to easily determine the cost-effectiveness of RES-P2P systems in Northern Europe.

First, an in-depth characterization (i.e., geographical position, number of inhabitants, key services, and current electrification system) and classification of the Norwegian islands was performed. Then, a multi-stage sorting procedure was conducted to identify the reference sites. A load estimation methodology (for both residential and non-residential buildings) was used to analyze the chosen sites, and a model was developed to estimate the renewable production. The sizing of the RES-P2P system was performed by using a techno-economic optimization tool with the aim of minimizing the LCOE while guaranteeing a reliable electricity supply. In order to carry out a comprehensive assessment of the different electrification strategies, the RES-P2P configuration was compared with alternative solutions based on the use of diesel generators or a submarine cable connection to the mainland grid, which is rarely investigated in literature. Finally, the environmental benefits, in terms of avoided fuel consumption and CO_2 emissions, were estimated and the results extrapolated for all 138 islands.

The structure of this paper is as follows: Section 2 provides a general overview of the Norwegian islands, presents the reference case studies and describes how the renewable energy production and electrical loads were estimated. It also presents the methodology for the optimal sizing of the renewable energy systems and the analysis of the alternative solutions. The main results of the techno-economic optimization are shown and discussed in Section 3. Finally, the conclusions are summarized in Section 4.

2. Methodology

2.1. Islands typologies and classification

Norway has about 50,000 islands (including islets and skerries), which vary greatly in distance from the mainland, population and size. Most islands are located near the coast, but some of them are in remote areas several kilometres from the mainland.

Depending on their size, islands can offer different services and facilities. For example, small islands usually do not have schools, stores or hospitals. In addition, Norwegian islands are usually connected to the mainland by ferries, so even providing essential commodities in more remote areas can be a challenge.

Depending on their location, islands pursue different strategies for energy supply: they can be powered by the national electric grid, through conventional transmission and distribution (T&D) systems or submarine cables, or they can rely on diesel generators. The analysis of the RES potential shows that a very abundant wind supply can be used near the cost and offshore. In contrast, the national average solar radiation is quite low compared to southern European countries. The distribution of the solar resource is almost uniform inland and along the coast, but is strongly influenced by latitudinal variations. Solbakken et al. [31] pointed out that the wind and solar resources have a complementary behaviour in Norway: in high-latitude areas, winter months are characterized by high wind speeds and almost no solar radiation, while the opposite is true in summer. Thus, the availability of wind and solar resources and the positive effects of their simultaneous exploitation make the installation of hybrid wind-PV systems attractive. Moreover, the variability of the electrical load and the fluctuating production of RES-based systems necessitate the use of energy storage solutions. As a result, there is a strong interest in renewable P2P systems, and an in-depth investigation is needed to evaluate the potential of this technology on a national scale. As a first step for this analysis, a census of the Norwegian islands was conducted to collect detailed information and create a database. The database developed in this study covers 495 Norwegian islands, sorted by county and municipality, and contains the following information:

1. the number of inhabitants based on the latest available data
2. geographical coordinates and area in km^2
3. a list of services offered on the island
4. notes (e.g., tourism, holiday homes, nature reserve status)
5. an indication of the current electrification system (submarine cable, T&D, local infrastructure or off-grid, which could be potentially based on diesel generators)
6. information on the submarine cable (length and year of installation).

Population data and geographical information were taken from Store Norske Leksikon website [32], while the services offered on the islands were evaluated based on GIS and cartographic observations. Finally, information on current electrification was taken from the Norwegian Water Resources and Energy Directorate online tool [33].

A multi-step sorting procedure was used to identify the most suitable sites for this analysis. First, 342 islands with reliable population data were identified, then 266 locations with less than 1000 inhabitants were selected (since islands with larger population are usually located near the coast and connected to the mainland with existing infrastructure). Finally, excluding islands with direct connection to T&D system, 138 potential sites were pinpointed and classified into 4 typologies based on the major services (i.e., shop, school and kindergarten) locally provided.

This classification was further refined by the introduction of a population range indicator, resulting in the identification of 10 subcategories, as shown in Table 1.

For each subcategory, a reference island was selected to perform the detailed techno-economic assessment. The chosen case studies cover the wide range of island typologies in terms of location, population and facilities. Moreover, each reference island is well representative of the different locations included in the subcategory: typically, in each group the minimum and maximum population and electrical load vary within a factor 2 compared to the reference location.

Table 1
Islands typologies and classification.

Typology	Population range	Reference island	Population of the reference island	Represented islands
No service	<50	Støttvær	27	41
	>50	Linesøya	77	19
1 shop	<100	Selvær	55	13
	>100	Lurøya	138	9
1 shop, 1 school	<200	Møkster	53	16
	200–400	Lepsøya	313	12
	>400	Røst	498	8
1 shop, 1 school, 1 kindergarten	<100	Rovær	86	2
	100–350	Skrova	196	9
	>350	Værøya	640	9

2.2. Layout of the hybrid renewable energy system

The RES-P2P system under analysis consists of the following components: solar PV, on-shore wind turbine (WT), battery (BT), electrolyzer (EL), hydrogen tank (HT) and fuel cell (FC). The Li-ion technology was considered for the battery component and the proton exchange membrane (PEM) technology was chosen for both the electrolyzer and fuel cell. A layout of the RES-based energy system with hybrid storage (i.e., battery and hydrogen) is shown in Fig. 1.

2.3. Electrical load estimation

2.3.1. Residential electrical load

Most of the models available in the literature do not fit the Norwegian case study due to the particular environmental conditions and living standards. In fact, more than 50% of Norwegian dwellings are detached houses with direct electric heating (often coupled with wood burning stoves or air-to-air heat pumps) [34]. Moreover, as is common in the Nordic countries in winter, day length has a significant impact on electricity consumption for lighting purposes. Therefore, a specific model was developed to estimate the electrical load of a reference residential building. The characteristics of the reference building were taken from [35] and are summarized in Table 2.

The model combined the monthly average consumption (Fig. 2a) of a detached house located in Ås (Norway) with the daily profile (Fig. 2b) of a remote household in southern Norway [35,36]. With the goal of obtaining an hourly-based load profile over the year for the reference building, the load estimation model properly rescaled the daily load profile of the remote household while preserving the monthly energy consumption of the detached house. Specifically, the daily load pattern was scaled up or down for each month according to the ratio between the daily average electrical load of the detached house (e.g., 4.50 kW in January and 1.17 kW in July) and the average daily electricity demand of the remote household (i.e., 2.28 kW). According to this procedure, the model generated a basic daily load profile for each month (Fig. 2c).

Moreover, the *day-to-day* (δ_{day}) and the *timestep-to-timestep* ($\delta_{timestep}$)

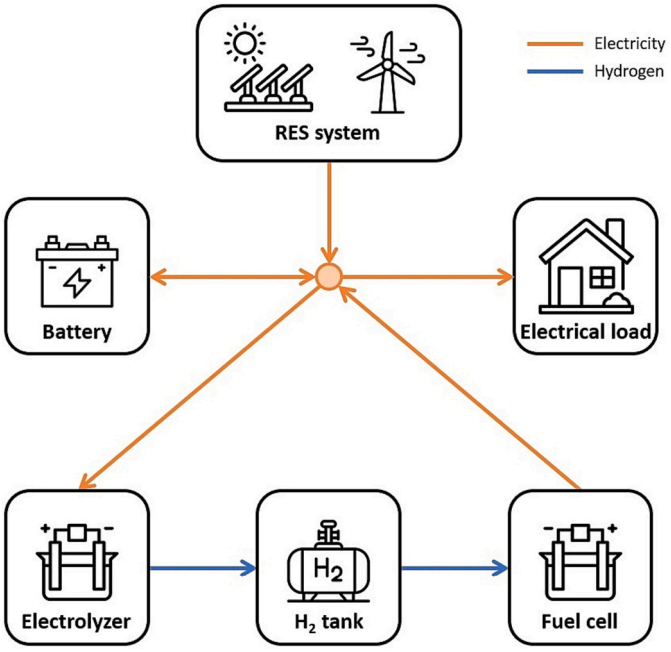

Fig. 1. Layout of the RES-P2P energy system.

Table 2
Specifications of the reference residential building.

Characteristic	Value
Dwelling type	Detached house
Number of residents	2 adults, 2 children
Floor area	150 m^2
Building year	< 1980
Heating source	100% electric

perturbation factors were introduced to make the profile more realistic [37]. The day-to-day perturbation determines the random daily variation of the size of the load profile while leaving the shape unchanged (i.e., the load profile is shifted upwards or downwards). On the contrary, the timestep-to-timestep perturbs the shape of the profile without affecting its size. Specifically, at each time step, the basic load profile was multiplied by a correction factor defined as follows:

$$\alpha(t) = 1 + \delta_{day}(d) + \delta_{timestep}(t) \quad (1)$$

The δ_{day} factor is randomly evaluated once per day (d) from a normal distribution with mean value equal to zero and standard deviation set to the daily variability index (I_{day}), while the $\delta_{timestep}$ factor is randomly generated once per hour (t) according to a normal distribution with mean value equal to zero and standard deviation equal to the timestep variability index ($I_{timestep}$). In this analysis, the I_{day} and $I_{timestep}$ variability indices were assumed equal to 12% and 5%, respectively [35]. Thus, both the size and the shape of the basic load profile were modified generating a variable electricity consumption profile (Fig. 2d).

As shown in Fig. 2d, the load profile of the reference building exhibits clear seasonality, with the highest consumption occurring in winter due to the combined effects of space heating and lighting demands.

Based on the permanent population (Table 1) and the number of occupants per building (Table 2), the number of houses on each island was estimated. The residential electrical load of the island was then determined by generating a load profile for each building and summing the different contributions.

2.3.2. Non-residential electrical load

The load profiles of non-residential buildings were estimated using the regression model proposed by Lindberg et al. [38]. The model takes into account the specific features of the building and includes the effect of outdoor temperature (hourly value and 24-hour moving average). Based on the outdoor temperature and building dimensions, the model can predict the electricity and heat consumption for lighting, electric appliances, space heating and water heating. In this study, it was assumed that the heat demand is met by electricity (e.g., direct electric systems and/or electric boilers) since this source is the most commonly used for heating purposes in Norway, even in non-residential buildings, as reported by Santori et al. [39]. The model was applied to determine the hourly load profiles of shops, schools and kindergartens for the different day types (i.e., weekday, weekend and holiday).

In Norway, kindergartens are open 10 hours per day and 5 days per week (also during summer), while schools operate 7–8 hours per day and 5 days per week (not during summer) [40]. The resulting annual specific energy consumption of kindergartens and schools is 179 kWh/m^2 and 149 kWh/m^2, respectively. These values are consistent with data from SINTEF and Statistics Norway [40,41]. The annual energy demand of shops turns out to be 202 kWh/m^2, which is in line with the data from Statistics Norway [41].

2.4. Estimation of the RES production

2.4.1. PV power plant

The meteorological data for PV power production estimation were extracted from the Photovoltaic Geographical Information System (PVGIS) tool considering the dataset for the Typical Meteorological Year (TMY) [42]. At each time interval t, the PV power production was evaluated as follows [43]:

$$P_{PV}(t) = f_{PV} \cdot P_{PV,rated} \cdot \left(\frac{G_T(t)}{G_{STC}}\right) \cdot \left[1 + \alpha_P \cdot \left(T_c(t) - T_{c,STC}\right)\right] \quad (2)$$

where P_{PV} (in kW) is the output power of the PV system, $P_{PV,rated}$ (in kW) is the rated power of the PV system, G_T (in kW/m^2) is the incident solar radiation evaluated for the optimal configuration of tilt and azimuth angles, G_{STC} (in kW/m^2) is the solar irradiance at standard test conditions (STC), T_c (in °C) is the actual PV cell temperature during operation, $T_{c,STC}$ (in °C) is the cell temperature at standard test conditions, α_P (in 1/K) is the temperature coefficient of power, and f_{PV} is the derating factor.

The PV cell temperature T_c (in °C) was expressed as [44]:

$$T_c(t) = T_a(t) + G_T(t) \cdot \left(\frac{T_{c,NOCT} - T_{a,NOCT}}{G_{T,NOCT}}\right) \cdot \left(1 - \frac{\eta_c}{\tau\alpha}\right) \quad (3)$$

where T_a (in °C) is the ambient temperature, $T_{c,NOCT}$ (in °C) is the cell temperature at nominal conditions, $T_{a,NOCT}$ (in °C) is the ambient temperature at nominal conditions, $G_{T,NOCT}$ (in kW/m^2) is the solar irradiance at nominal conditions, η_c is the PV cell efficiency and $\tau\alpha$ is the product of the solar transmittance and absorbance.

The PV cell efficiency was assessed according to the following expression:

$$\eta_c = \eta_{c,STC} \cdot \left[1 + \alpha_P \cdot \left(T_c(t) - T_{c,STC}\right)\right] \quad (4)$$

where $\eta_{c,STC}$ is the PV cell efficiency at standard test conditions.

2.4.2. Wind power plant

At each time interval t, the power production of the wind turbine (WT) system was determined by using the following power curve relationship [29]:

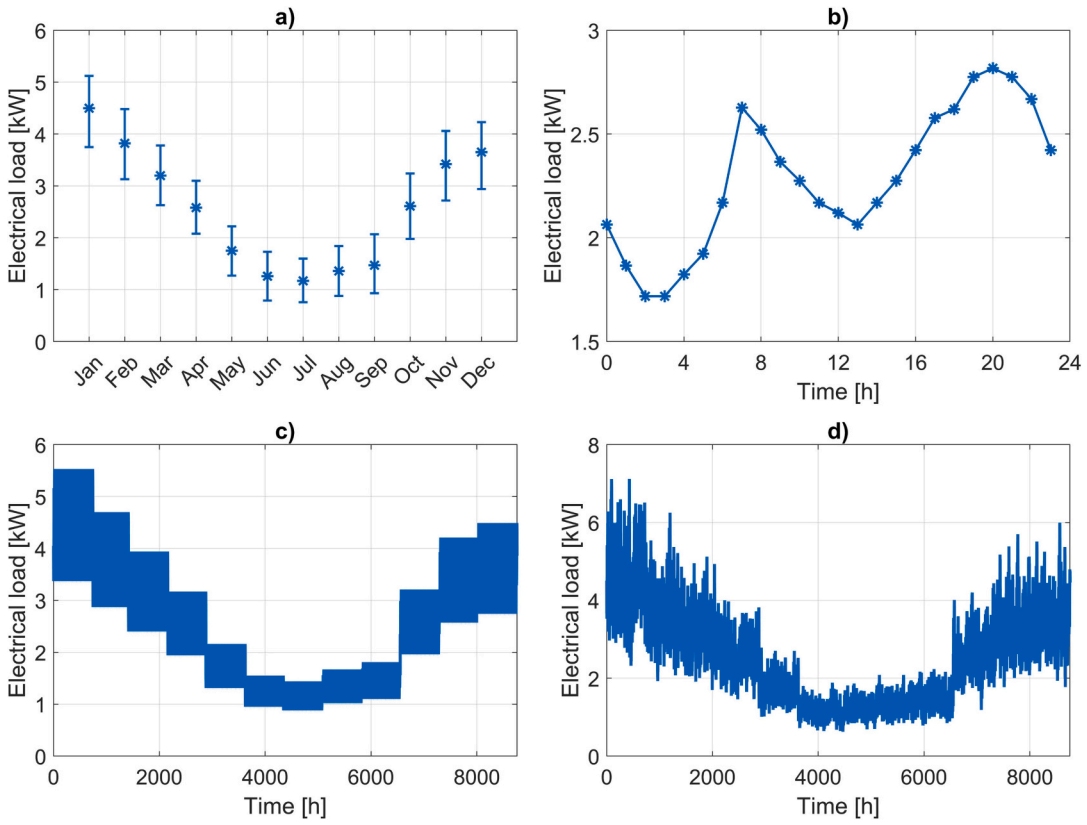

Fig. 2. a) Monthly average electricity consumption of a detached house; b) daily load profile of a remote house in southern Norway; c) single house basic load profile; d) single house realistic load profile.

$$P_{WT,std}(t) = \begin{cases} 0, & if\ u_w(t) < u_{w,ci} \\ P_{WT,rated} \cdot \left(\dfrac{u_w^3(t) - u_{w,ci}^3}{u_{w,r}^3 - u_{w,ci}^3} \right), & if\ u_{w,ci} < u(t) < u_{w,r} \\ P_{WT,rated}, & if\ u_{w,r} < u(t) < u_{w,co} \\ 0, & if\ u_w(t) > u_{w,co} \end{cases} \quad (5)$$

where $u_{w,r}$, $u_{w,ci}$ and $u_{w,co}$ (in m/s) are the rated, cut-in and cut-off wind speed, respectively. $P_{WT,rated}$ (in kW) is the WT rated power and $P_{WT,std}$ (in kW) is the WT output power at standard conditions.

Wind speed values were taken from PVGIS [42] and are available at a reference height (h_{ref}) of 10 m. Therefore, a power law correction was applied to determine the corresponding wind speed values at the hub height (h_{hub}) [45]:

$$u_w(t) = u_{wind,ref}(t) \cdot \left(\frac{h_{hub}}{h_{ref}} \right)^{\alpha} \quad (6)$$

To account for the effect of ambient temperature on the wind turbine power, the output power at standard conditions was adjusted as follows:

$$P_{WT}(t) = P_{WT,std}(t) \frac{\rho_{air}(t)}{\rho_{air,std}} \quad (7)$$

where ρ_{air} (in kg/m^3) is the actual air density (which was evaluated based on the hourly values of air temperature and ambient pressure extracted from PVGIS [42]) and $\rho_{air,std}$ (in kg/m^3) is the air density at standard conditions.

The main technical parameters for the estimation of the PV and WT power are summarized in Table 3.

Table 3
Main technical parameters of the PV and WT systems.

Component	Value	Ref.
PV panel		
Derating factor, f_{PV}	0.86	[42]
Cell efficiency at STC, $\eta_{c,STC}$	0.21	[46]
Temperature coefficient of power, α_P	−0.003 1/K	[46]
Nominal operating temperature, $T_{c,NOCT}$	44 °C	[46]
Solar transmittance and absorbance, $\tau\alpha$	0.9	[44]
Solar irradiance at STC, G_{STC}	1 kW/m^2	
Cell temperature at STC, $T_{c,STC}$	25 °C	
Solar irradiance at nominal conditions, $G_{T,NOCT}$	0.8 kW/m^2	
Ambient temperature at nominal conditions, $T_{a,NOCT}$	20 °C	
Wind turbine		
Turbine height, h_{hub}	30 m	[47]
Cut-in wind speed, $u_{w,ci}$	3 m/s	[47]
Cut-off wind speed, $u_{w,co}$	25 m/s	[47]
Rated wind speed, $u_{w,r}$	13 m/s	[47]
Power law coefficient, α	1/7	[48]
Air density at standard conditions, $\rho_{air,std}$	1.225 kg/m^3	

2.5. Optimal sizing of the stand-alone renewable energy system

2.5.1. Energy management strategy

An energy management strategy (EMS) has been defined to regulate the operation of the RES-P2P system in order to improve the exploitation of local renewable energy sources and reliably meet the load demand. In this work, the EMS regulates the operation of the system based on the state of charge (SOC) of the storage devices and the modulation range of

the different components.

The battery state of charge is defined as the ratio between the energy stored within the battery and its rated capacity. At each time interval t, it was evaluated according to the following expression:

$$SOC_{BT}(t) = SOC_{BT}(t-1) + \frac{P_{BT,ch}(t-1)\cdot\Delta t\cdot\eta_{BT,ch}}{Cap_{BT}} - \frac{P_{BT,dc}(t-1)\cdot\Delta t}{\eta_{BT,dc}\cdot Cap_{BT}} \quad (8)$$

where $P_{BT,ch/dc}$ (in kW) is the charging/discharging power of the battery, $\eta_{BT,ch/dc}$ is the charging/discharging efficiency of the battery, Cap_{BT} (in kWh) is the rated capacity of the battery and Δt is the time resolution (1 h in this analysis).

The battery SOC can range between a minimum and maximum value as follows:

$$SOC_{BT,min} \le SOC_{BT}(t) \le SOC_{BT,max} \quad (9)$$

The $SOC_{BT,min}$ value was imposed in order to avoid excessive battery discharge and limit battery degradation and failures [49].

Analogously to the battery, the state of charge of the hydrogen tank (SOC_{HT}) is defined as the ratio between the energy stored in the hydrogen tank and its rated capacity. It was computed as follows:

$$SOC_{HT}(t) = SOC_{HT}(t-1) + \frac{P_{EL}(t-1)\cdot\Delta t\cdot\eta_{EL}}{Cap_{HT}} - \frac{P_{FC}(t-1)\cdot\Delta t}{\eta_{FC}\cdot Cap_{HT}} \quad (10)$$

where $P_{EL/FC}$ (in kW) is the electrolyzer/fuel cell operating power, $\eta_{EL/FC}$ is the electrolyzer/fuel cell efficiency and Cap_{HT} (in kWh) is the rated capacity of the hydrogen tank.

The variation of the SOC_{HT} value was bounded between a lower and upper limit as reported below:

$$SOC_{HT,min} \le SOC_{HT}(t) \le SOC_{HT,max} \quad (11)$$

The $SOC_{HT,min}$ value was calculated as the ratio between the minimum and maximum pressure of the hydrogen tank. This constraint on the minimum SOC value was set so that hydrogen can be fed into the fuel cell without the need for additional auxiliary equipment. Moreover, it was assumed that the electrolyzer operates under pressurized conditions (30 bar) to avoid the installation of a compressor between the electrolyzer and the hydrogen tank (whose maximum pressure is 28 bar).

The electrolyzer and fuel cell were imposed to work within a certain modulation range to ensure a safe and efficient operation. The main input parameters of the energy management strategy are listed in Table 4.

Table 4
Input parameters of the energy management strategy.

Component	Value	Reference
Li-ion battery		
Charging efficiency, $\eta_{BT,ch}$	0.95	[50]
Discharging efficiency, $\eta_{BT,dc}$	0.95	[50]
Minimum SOC, $SOC_{BT,min}$	0.2	[49,50]
Maximum SOC, $SOC_{BT,max}$	1	
PEM electrolyzer		
Efficiency (LHV)	58%	[28]
Modulation range (% of rated power)	10%–100%	[28]
PEM fuel cell		
Efficiency (LHV)	47%	[28]
Modulation range (% of rated power)	6%–100%	[28]
Hydrogen tank		
Minimum pressure, p_{min}	3 bar	[28]
Maximum pressure, p_{max}	28 bar	[28]
Minimum SOC, $SOC_{HT,min}$	p_{min}/p_{max}	
Maximum SOC, $SOC_{HT,max}$	1	

According to the adopted EMS, the battery component has the priority of intervention and its SOC parameter is the main decision factor of the EMS. Specifically, whenever the RES production exceeds the electrical load, the battery system is first charged until the $SOC_{BT,max}$ value is reached. Then, the excess renewable electricity is converted to hydrogen by the electrolyzer until the hydrogen tank is full, and finally curtailed (if necessary). When the electrical demand is higher than the RES production, first the battery bank is discharged until its minimum SOC is reached, and then the fuel cell is turned on to meet the remaining power shortage. In this way, the battery is given priority due to its high efficiency and fast response. This control strategy is also effective in limiting the number of times the electrolyzer and fuel cell are turned on and off, thus mitigating their performance degradation over time. The detailed flowchart of the adopted EMS can be found in [28].

The energy simulations were performed over a reference year with hourly time resolution, which represents a good trade-off between the accuracy of the results and the computational burden [51].

2.5.2. Techno-economic optimization

The design of the RES-P2P system was performed using a techno-economic optimization tool based on a two-layer approach. In the outer layer, the particle swarm optimization (PSO) algorithm is used to determine a possible system configuration, while in the inner layer, the system operation is managed according to the EMS described in Section 2.5.1 [21]. PSO represents one of the most widely adopted metaheuristic algorithms for the optimal design of renewable energy systems. PSO results easier to implement than other optimization techniques (e.g., genetic algorithm) since it requires fewer parameters to be tuned [52]. Moreover, it exhibits high convergence speed also for problems with several design variables [53] and it proved to be slightly less dependent on the initial solution compared to alternative metaheuristic schemes [54]. PSO is thus characterized by strong convergence and robustness [55].

The optimal sizing consists in identifying the system configuration that minimizes the LCOE while satisfying the constraints (13) and (14).

The reliability of the RES-based energy system was assessed through the loss of power supply probability (LPSP) index. It represents the annual fraction of the electrical demand that cannot be met by the system and is defined according to the following expression:

$$LPSP = \sum_{t=1}^{N_t} \frac{P_{deficit}(t)\cdot\Delta t}{P_{load}(t)\cdot\Delta t} \quad (12)$$

where P_{load} (in kW) is the electrical load to cover, $P_{deficit}$ (in kW) is the electrical load not covered by the energy system, Δt is the time resolution (1 h) and N_t is the number of time intervals over the year (8760). A constraint was imposed on the LPSP index as follows:

$$LPSP \le LPSP_{target} \quad (13)$$

In this study, the $LPSP_{target}$ was set to zero to ensure the complete energy autonomy of the islands.

As shown in Eq. (14), the size of the i-th component (S_i) of the energy system can range between zero and an upper bound (with i = PV, WT, BT, EL, FC, HT):

$$0 \le S_i \le S_{i,max} \quad (14)$$

For each component, the upper bound was set high enough not to be a constraint on the optimal design process. The $S_{i,max}$ values of the hydrogen components (i.e., EL, HT and FC) were set to zero in the analysis of the battery-only scenario (i.e., a scenario with only batteries as energy storage).

The LCOE (in €/kWh), which is the objective function of the optimization process, was evaluated as follows:

$$LCOE = \frac{C_{NPC,tot}}{\sum_{j=1}^{L_{PR}} \frac{E_{tot,j}}{(1+d)^j}} \quad (15)$$

where $C_{NPC,tot}$ (in €) is the total net present cost of the system, $E_{tot,j}$ (in kWh) is the electrical demand covered by the RES-P2P system in the j-th year and L_{PR} is the lifetime of the project (assumed to be equal to 20 years). The real discount rate d, which is a function of the nominal discount rate and the annual inflation rate, was set equal to 4.9% [28].

As reported in Eq. (16), the total net present cost includes the investment costs, the operation and maintenance (O&M) costs and the replacement costs incurred over the lifetime of the project (with i = PV, WT, BT, EL, FC, HT):

$$C_{NPC,tot} = \sum_i C_{inv,i} + \sum_{j=1}^{L_{PR}} \left(\frac{\sum_i C_{O\&M,i,j}}{(1+d)^j} + \frac{\sum_i C_{rep,i,j}}{(1+d)^j} \right) \quad (16)$$

where $C_{inv,i}$ (in €) is the investment cost of the i-th component at the beginning of the analysis period, $C_{O\&M,i,j}$ and $C_{rep,i,j}$ (in €) are the O&M and replacement costs of the i-th component during the j-th year, respectively. The cost of replacing a certain component takes place at the end of its lifetime and only if this value is lower than the lifetime of the project.

The techno-economic data required for the LCOE assessment are listed in Table 5.

Table 5
Economic input data of the RES-P2P system.

Component	Value	Reference
PV power plant		
Investment cost	1547 €/kW	[28]
Fixed O&M	24 €/(kW·yr)	[28]
Lifetime	Project lifetime	
Wind power plant		
Investment cost	1175 €/kW	[56]
Fixed O&M (% of inv. cost)	3%/yr	[28]
Lifetime	Project lifetime	
Li-ion battery		
Investment cost (system)	550 €/kWh	[28,49]
Replacement cost (module)	350 €/kWh	
Fixed O&M	10 €/(kWh·yr)	[57]
Module lifetime	Lifetime curve	[21]
Lifetime (except for the modules)	Project lifetime	
PEM electrolyzer		
Ref. specific investment cost, $c_{inv,ref}$	4600 €/kW	[58]
Ref. rated size, $P_{rated,ref}$	50 kW	[58]
Cost exponent, n	0.65	[58]
Replacement cost of stack (% of inv. cost)	26.7%	[59]
Fixed O&M (% of inv. cost)	(1/3)·4%/yr	[60]
Variable O&M (% of inv. cost)	(2/3)·4%/yr	[60]
Operating hours of the stack (over lifetime)	40,000 h	[60]
On-off cycle numbers of the stack (over lifetime)	5000	[61]
Lifetime (except for the stack)	Project lifetime	
PEM fuel cell		
Ref. specific investment cost, $c_{inv,ref}$	3947 €/kW	[62]
Ref. rated size, $P_{rated,ref}$	10 kW	[62]
Cost exponent, n	0.7	[21]
Replacement cost of the stack (% of inv. cost)	26.7%	[59]
Fixed O&M (% of inv. cost)	(1/3)·4%/yr	[60]
Variable O&M (% of inv. cost)	(2/3)·4%/yr	[60]
Operating hours of the stack (over lifetime)	30,000 h	[48,63]
On-off cycle numbers of the stack (over lifetime)	10,000	[64]
Lifetime (except for the stack)	Project lifetime	
Hydrogen tank		
Investment cost	470 €/kg	[60]
Fixed O&M (% of inv. cost)	2%/yr	[60]
Lifetime	Project lifetime	

The following power function was used to estimate the investment cost of the electrolyzer and fuel cell:

$$c_{inv} = \left(\frac{P_{rated}}{P_{rated,ref}} \right)^n \cdot \frac{c_{inv,ref} \cdot P_{rated,ref}}{P_{rated}} \quad (17)$$

where c_{inv} (in €/kW) is the specific investment cost of the component with size P_{rated} (in kW), $c_{inv,ref}$ (in €/kW) is the specific investment cost of the component with reference size $P_{rated,ref}$ (in kW) and n is the cost exponent of the power function. Eq. (17) was applied to consider the effect of size on the costs of hydrogen-based devices. This effect is indeed significant in the kW-size range. The resulting cost values are in accordance with those of the REMOTE project and with costs of kW-size electrolyzers and fuel cells [28].

The O&M costs of the fuel cell and electrolyzer were set equal to 4% of their investment cost. They include a fixed and a variable contribution accounting for 1/3 and 2/3, respectively [60]. It was assumed that the variable O&M term is proportional to the operating hours of the fuel cell/electrolyzer over the year.

In this study, the lifetime of the battery modules, fuel cell stack and electrolyzer stack were evaluated based on the energy simulation of the RES-P2P system. These values are needed in the LCOE assessment to estimate when replacement costs will be incurred during the project lifetime. Specifically, battery module lifetime was estimated as the ratio between lifetime throughput (LT) and annual throughput (AT) [21]. The LT parameter represents the total amount of energy that can flow through the battery during its lifetime and can be derived from the battery lifetime curve. The AT parameter, on the other hand, stands for the energy flowing through the battery during one year, and thus depends on the operation of the RES-P2P system. The lifetime of the fuel cell and electrolyzer stacks was estimated by comparing their annual number of operating hours and start-ups (which depends on the energy simulation of the RES-P2P system) with their lifetime number of operating hours and start-ups (which are reported in Table 5) [21].

2.6. Alternative scenarios

Connection to the mainland grid by submarine cables (SCs) and the use of diesel generators were considered as alternative solutions for the electricity supply of the islands.

In the submarine cable scenario, the NPC was computed using the following equation:

$$C_{NPC} = C_{inv,SC} + \sum_{j=1}^{L_{PR}} \left(\frac{C_{O\&M,SC,j}}{(1+d)^j} + \frac{E_{tot,j} \cdot c_{grid}}{(1+d)^j} \right) \quad (18)$$

where $C_{inv,SC}$ (in €) is the investment cost of the submarine cable, $C_{O\&M,SC,j}$ (in €) is the submarine cable O&M cost in the j-th year and c_{grid} (in €/kWh) is the cost of purchasing electricity from the national grid. The CAPEX of the submarine connection was assumed to be dependent only on the cable length, which represents the most impactful parameter for the investment cost. In this scenario, the investment and operating expenditures were estimated based on the real costs provided by the REMOTE project partner TrønderEnergi [65]. Details are omitted for confidentiality reasons, but the specific investment cost (€/km) derived from the Froan demo site is in line with other studies carried out in Norway [66,67].

The NPC of the diesel-based scenario was derived as follows:

$$C_{NPC} = C_{inv,DG} + \sum_{j=1}^{L_{PR}} \left(\frac{C_{O\&M,DG,j}}{(1+d)^j} + \frac{C_{rep,DG,j}}{(1+d)^j} \right) \quad (19)$$

Table 6
Techno-economic parameters of diesel generator.

Parameter	Value	Reference
Investment cost	420 €/kW	[49]
Replacement cost	420 €/kW	[49]
Price of diesel fuel	2 €/L	[8,49]
Fuel consumption curve parameter, a_{DG}	0.08415 L/kWh	[29]
Fuel consumption curve parameter, b_{DG}	0.246 L/kWh	[29]
Minimum power (% of rated power)	30%	[68]
CO_2 emission coefficient	3 kg/L	[69]
Operating hours over lifetime	16,000 h	[28]

where $C_{inv,DG}$ (in €) is the investment cost for the diesel generator, whose size was determined based on the peak load demand. $C_{O\&M,DG,j}$ and $C_{rep,DG,j}$ (in €) are the O&M and replacement costs of diesel generator in the j-th year, respectively. The lifetime of the diesel generator was calculated by comparing its lifetime hours (see Table 6) with its annual operating hours (which depend on the energy simulation of the energy system). The O&M expenditures were derived from the annual diesel fuel consumption. At each time step t, the fuel consumed $cons_{DG}$ (in L/h), was assessed according to the following consumption curve:

$$cons_{DG}(t) = a_{DG} \cdot P_{DG,rated} \cdot \delta_{DG}(t) + b_{DG} \cdot P_{DG}(t) \quad (20)$$

where $P_{DG,rated}$ and P_{DG} (in kW) are the DG rated power and the operating power, respectively. The δ_{DG} term is a binary variable introduced to model the on/off status of the genset (i.e., it is equal to 1 when the DG is producing electricity and 0 otherwise). According to Eq. (20), the fuel consumption is null when no electricity is produced: indeed, if P_{DG} is equal to zero also δ_{DG} is zero and thus no fuel is consumed.

In modelling the genset operation, a minimum operating power was imposed (30% of the rated power) to prevent the system from running at too low efficiency [68].

In remote areas, the fuel price can be strongly affected by transportation costs. For this reason, a diesel price of 2 €/L was considered in this study [8,49]. The annual CO_2 emissions caused by the diesel generators were calculated in agreement with Jakhrani et al. [69], using an emission factor equal to 3 kg/L. The main techno-economic parameters of the diesel scenario are reported in Table 6.

Eq. (15) was then employed to derive the LCOE of the submarine cable and diesel scenarios.

3. Results and discussion

The optimal sizing of the RES-P2P system was performed for the 10 islands identified in Section 2.1. The main characteristics of the islands are summarized in Table 7. The annual energy consumption and peak demand were determined by applying the load estimation models presented in Section 2.3.

As shown in Table 7, submarine cables are widely adopted for both nearshore and remote islands. However, the outdated connections need to be replaced in the near future, and alternatives have to be found to avoid the costly installation of submarine cables or the use of diesel generators [70]. By combining local RES and energy storage, RES-P2P systems can be a solution to ensure power supply to the islands.

The main sizing results of the RES-P2P systems are shown in Table 8. The majority of the installed RES capacity is represented by the wind technology. However, the installation of hybrid PV-wind systems turns out to be profitable due to the complementary seasonality of wind speed and solar radiation. Moreover, it is worth noting that, due to the seasonal variation of the electrical load, hydrogen plays a pivotal role in providing long-term energy storage. A large storage capacity is thus necessary to ensure the energy self-sufficiency of the islands.

Fig. 3 shows the energy balances obtained by processing the results of the annual simulations. As evidenced in Fig. 3a, renewable electricity generation can directly cover more than 75% of the annual electrical load, while the remaining demand is met by the hybrid energy storage solution: typically more than 15% by fuel cells and less than 10% by batteries. The hydrogen-battery storage is thus crucial to move towards a 100% RES-based energy system. Fig. 3b shows how the annual available RES energy is exploited and distributed between the load (i.e., direct consumption), the battery, the electrolyser (in the form of hydrogen), or curtailed. It is noteworthy that on all the islands, roughly 50% (or more) of the total renewable energy has to be curtailed, as typically occurs in off-grid energy systems that aim to rely entirely on local RES [71].

The resulting LCOE values of the RES-P2P solution are shown in Fig. 4, which also highlights the contribution of the different components to the total LCOE. It can be seen that the LCOE is in the range of 0.21 to 0.63 €/kWh.

When analyzing the LCOE breakdown, the largest contributions come from the wind turbines and the hydrogen-based components (i.e., EL, HT and FC), while the PV and battery components have a limited impact since their sizes are small (and even negligible for some islands). In fact, the capacity of the battery is always less than 280 kWh, as it mainly acts as a short-term storage to compensate for the daily fluctuations of renewable power. Instead, the HT capacity reaches values of up to about 170 MWh (e.g., on the island of Værøya).

The influence of the RES availability on the LCOE was investigated in order to understand the reasons for the different electricity generation costs on the islands (0.21 to 0.63 €/kWh). The WT capacity factor (CF) parameter was thus introduced. It is defined (on a yearly basis) as the ratio between the WT electrical energy output and the maximum WT electrical energy output, as described by the following expression:

Table 7
Main characteristics of the reference islands.

Island	Island acronym	Number of houses	Annual energy consumption [kWh/yr]	Peak demand [kW]	Minimum ambient temperature [°C]	Average ambient temperature [°C]	Average wind speed at 10 m height [m/s]	Sea cable length [km]	Year of installation
Støttvær	STV	7	156,386	44.2	−3.3	8.6	5.1	2.8	1991
Linesøya	LNS	19	425,777	113.4	−18.8	6.8	4.36	3.8	1980
Selvær	SEL	14	345,976	86.5	−11.7	6.8	7.7	34[a]	–
Lurøya	LUR	35	861,179	218	−16.7	3.5	5.8	7.6[a]	–
Møkster	MOK	13	367,258	88.6	−1	8.7	6.6	1.2	1954
Lepsøya	LEP	78	2,030,630	472.7	−9.6	7.9	6.9	4.6	2011
Røst	ROS	125	3,213,030	758.6	−5.2	6.9	7.8	33.2	2009
Rovær	ROV	22	605,290	143.4	0.2	8.9	6.6	7.8	2005
Skrova	SKR	49	1,294,400	304.8	−8.1	5.7	6.7	9	1979
Værøya	VRY	160	4,279,804	985.2	−5.1	6.8	7.4	27.9	1986

[a] Currently, Selvær and Lurøya islands are not connected to the grid via sea cables. The cable lengths were assumed equal to their distance from the mainland.

Table 8
Main sizing results of the RES-P2P system for the 10 reference islands.

Island	PV [kW]	WT [kW]	EL [kW]	FC [kW]	HT [kWh]	BT [kWh]
Støttvær	3	341	53	40	6433	116
Linesøya	87	812	198	115	16,877	421
Selvær	10	244	69	85	12,744	72
Lurøya	7	1629	613	228	49,995	21
Møkster	39	307	105	90	17,981	142
Lepsøya	10	2177	1331	490	149,326	66
Røst	10	1888	791	775	94,499	280
Rovær	30	517	181	143	35,179	160
Skrova	82	1095	226	301	37,760	18
Værøya	235	2991	894	944	169,126	20

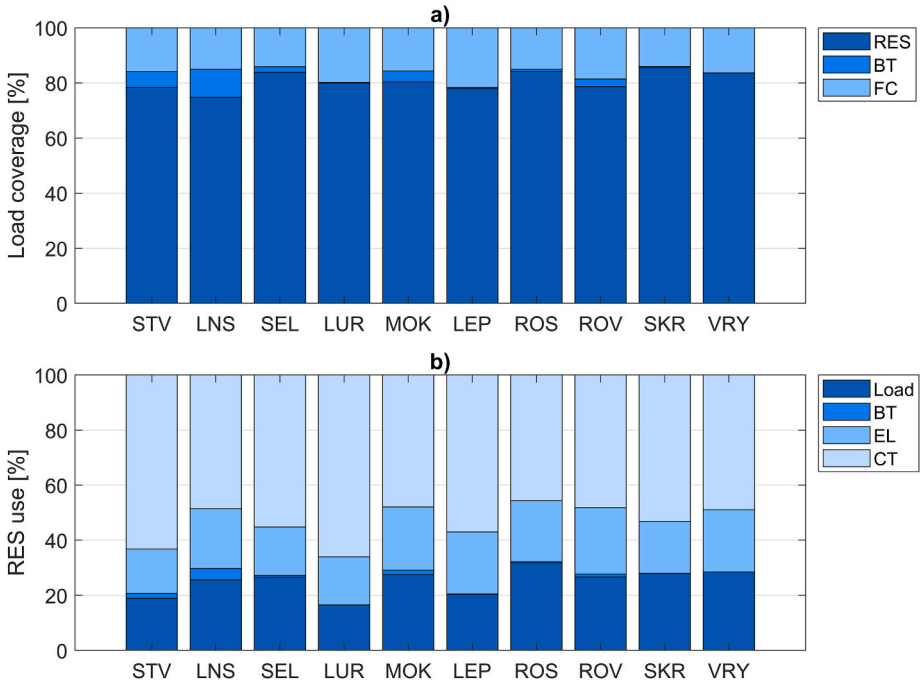

Fig. 3. a) Coverage of the electrical load (on an annual basis) and b) RES use (on an annual basis) for the 10 reference islands.

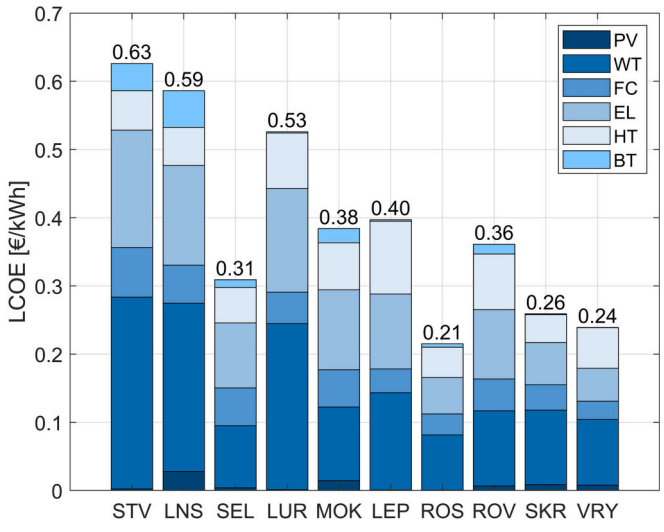

Fig. 4. LCOE breakdown of the RES-P2P system for the 10 reference islands.

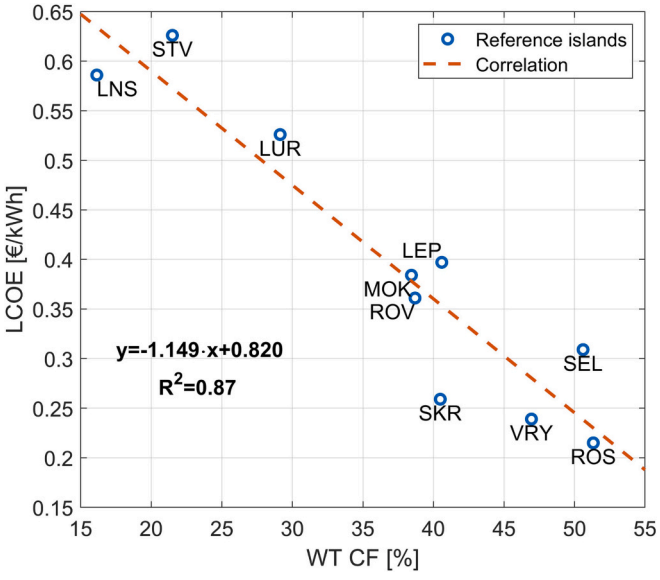

Fig. 5. LCOE as a function of the WT capacity factor.

Table 9
Main sizing results of the RES-P2P system with only batteries as energy storage.

Island	PV [kW]	WT [kW]	BT [kWh]	LCOE [€/kWh]
Støttvær	10	486	2245	1.18
Linesøya	162	1184	4091	0.91
Selvær	5	641	5030	1.02
Lurøya	5	2450	13,243	1.19
Møkster	410	569	3247	0.84
Lepsøya	10	5631	24,745	1.01
Røst	103	9237	10,210	0.55
Rovær	563	1000	9683	1.21
Skrova	712	1339	9469	0.61
Værøya	255	9685	21,029	0.56

$$CF_{WT} = \frac{\sum_{t=1}^{N_t} P_{WT}(t)\cdot\Delta t}{P_{WT,rated}\cdot\Delta t\cdot N_t} \quad (21)$$

where P_{WT} (in kW) is the WT electrical power, $P_{WT,rated}$ (in kW) is the WT rated power, Δt is the time resolution (1 h) and N_t is the number of time intervals over the year (8760).

On the Norwegian islands, wind power represents the most abundant and exploitable local RES, but its potential is quite unevenly distributed. This has a strong impact on the cost of electricity, as shown in Fig. 5, in which the LCOE is plotted as a function of the WT capacity factor. The cost of electricity decreases with increasing availability of the wind resource, showing a clear linear correlation (R^2 equal to 0.87). Specifically, the LCOE is around 0.6 €/kWh when the capacity factor is close to 20% and decreases to almost 0.2 €/kWh when the capacity factor is above 50%, as in the case of Røst island. The derived correlation can be thus adopted to readily estimate the LCOE of RES-P2P systems in Norway. Moreover, it emphasizes that a high wind availability is crucial for improving the cost-effectiveness of these systems.

In order to better assess the role of hydrogen, a scenario with only batteries as energy storage was investigated. For this purpose, the $S_{i,max}$ value of the hydrogen-based components was set to zero (see Eq. (14)). The main results of the optimal sizing process for the only-battery scenario are reported in Table 9.

Compared to a configuration with hybrid storage (Table 8), the only-battery system entails a significant increase in the sizes of the RES generators and battery storage, as also confirmed by Zhang et al. in [23]. The system oversizing and the high investment cost for batteries have a negative impact on the LCOE, which increases significantly from 0.21–0.63 €/kWh (hybrid storage) to 0.55–1.21 €/kWh (only-battery). As an example, in Møkster case study, the PV and WT rated power increase respectively by a factor 10 and 1.8, while the battery capacity is 23 times larger than that installed in the hybrid storage configuration. As a consequence, the LCOE abruptly rises from 0.38 to 0.84 €/kWh.

The presence of a hydrogen-based storage is thus crucial to achieve the lowest LCOE. Moreover, storage hybridization (i.e., both hydrogen and batteries) proves to be the most cost-effective solution since it can take advantage of both the high efficiency of batteries and the low-cost large storage capacity of hydrogen. Hydrogen helps prevent the system oversizing (RES generators and batteries) and provides long-term energy storage to cope with the seasonal variations in the electrical load. It is therefore fundamental to offer a reliable and cost-competitive 100% RES-based energy supply.

These considerations are further confirmed by Fig. 6, in which the SOC of battery and hydrogen storage is shown for the island of Linesøya. It can be noted that the batteries act as a short-term storage: the daily charging and discharging phases cope with the RES intermittency and compensate for the intraday fluctuations in the RES production. Conversely, the hydrogen SOC exhibits a clear seasonal behaviour, as it provides long-term energy storage. The pressurized tank is filled with hydrogen when abundant RES surplus is available (e.g., May and June), it is saturated during summer and is discharged when the electrical load on the island increases. The hydrogen tank capacity is about 40 times larger than that of the battery (16,877 kWh of hydrogen tank and 412 kWh of battery).

For the sake of comparison, submarine cable connection to mainland grid and diesel generators were considered as alternative solutions for the electricity supply to the islands. The resulting LCOE values are listed in Table 10.

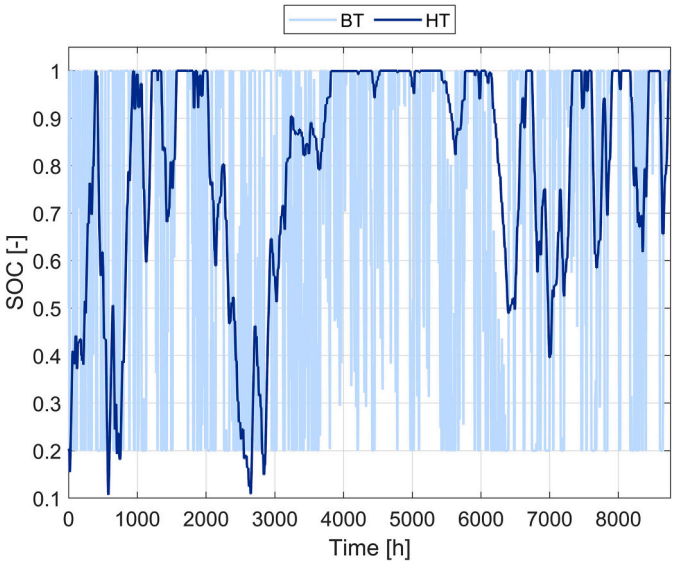

Fig. 6. SOC of battery and hydrogen storage for the island of Linesøya. (BT capacity = 421 kWh, HT capacity = 16,877 kWh).

Table 10
Main results of submarine cable and diesel-based scenarios.

Island	Submarine cable	Diesel	
	LCOE [€/kWh]	LCOE [€/kWh]	Direct CO_2 [t/yr]
Støttvær	0.35	1.04	225
Linesøya	0.23	0.92	503
Selvær	1.47	0.97	498
Lurøya	0.23	0.89	1005
Møkster	0.14	0.93	480
Lepsøya	0.14	0.88	2337
Røst	0.25	0.88	3693
Rovær	0.28	0.90	702
Skrova	0.20	0.88	1493
Værøya	0.20	0.87	4898

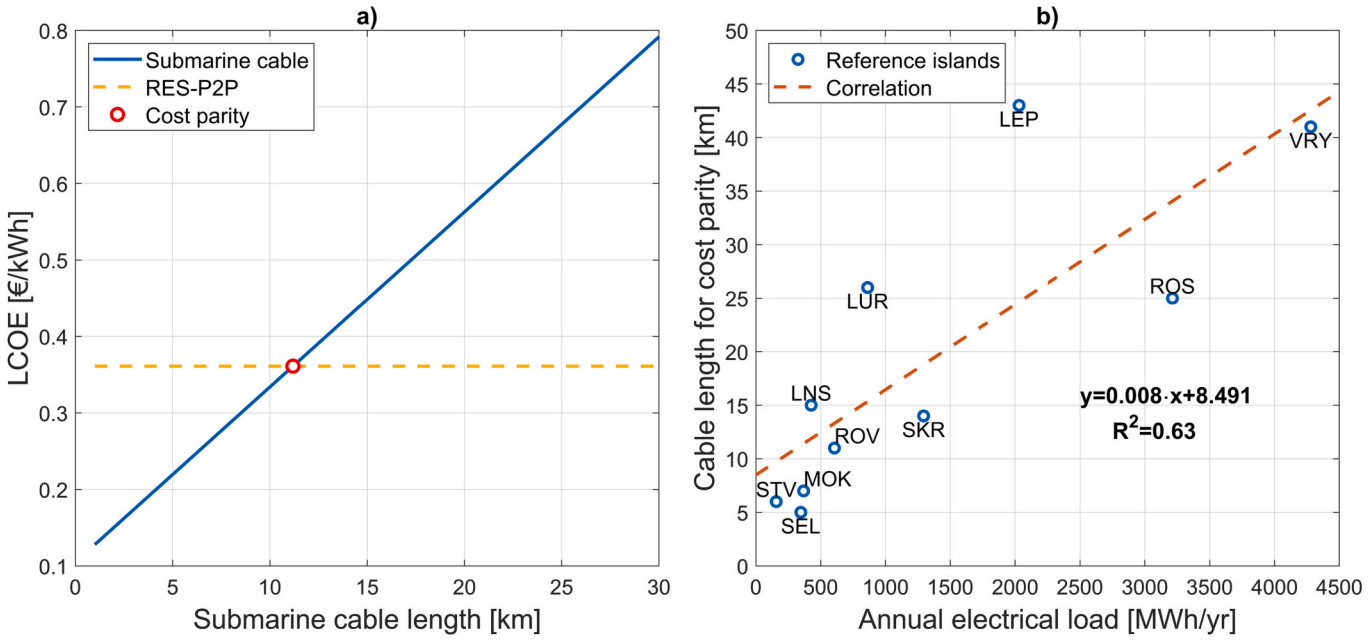

Fig. 7. a) Estimation of the cable length to achieve cost parity between the RES-P2P and the cable-based solutions; b) Cost-parity length of the submarine cable as a function of the annual electrical load for the 10 reference islands.

In the submarine cable scenario, the LCOE values are very different and range from 0.14 to 1.47 €/kWh. Fig. 7a explains graphically how to derive the length of the submarine cable to achieve cost parity between the RES-P2P and the cable-based solutions. As an illustrative example, it refers to the island of Rovær and shows that the cost parity is reached when the island is about 11 km from the mainland. Fig. 7b shows the cable length required to achieve the cost parity for the different reference islands. It also provides a generalization for the dependence of the cost-parity length on the annual electrical load. This correlation allows to easily compare the RES-P2P system with the cable solution based only on the distance from the mainland and the annual electrical consumption. The economic feasibility of the cable-based solution is strongly affected by the cable length and the electrical load of the islands. For small islands (with an annual electrical load below approximately 1500 MWh), the cable length (i.e., distance from the mainland) should be less than 5–15 km for the cable-based solution to be cheaper than the RES-P2P option. The cost-parity length increases as the annual electrical load increases. For example, on the island of Værøya, where the electricity demand is almost 4500 MWh per year, the cost parity is around 40 km. These results suggest that RES-P2P systems can be a cost-effective solution for the electrification of remote islands, especially for small sites located more than 5–15 km from the mainland.

As shown in Table 10, the LCOE for the diesel-based scenario is in the range of 0.87–1.04 €/kWh. The high cost of electricity production is mainly due to the operating costs associated with the diesel fuel consumption. This cost contribution increases further in remote locations where the fuel price can reach very high values because of transportation costs. Furthermore, fossil fuel-based electrification causes serious environmental impacts, as evidenced by the annual CO_2 emissions in Table 10. It is therefore clear that the use of diesel generators is neither a cost-competitive nor an environmentally friendly option.

A nationwide assessment was also performed to estimate the environmental benefits of installing RES-P2P systems on 138 Norwegian islands. In order to determine the overall reduction in CO_2 emissions compared to the diesel-based scenario, the results of the 10 reference case studies were extrapolated for all the potential installation sites. More specifically, for each island in the database, fuel consumption and CO_2 emissions were estimated by scaling the corresponding values of the reference island up or down (depending on the number of inhabitants). The environmental analysis shows that the installation of the RES-P2P system on 138 islands can result in a saving of about 184 kt_{CO2} per year (corresponding to $61 \cdot 10^6$ litres of diesel fuel).

4. Conclusions

The potential for installing RES-based hydrogen-battery systems for sustainable electrification of remote islands in Norway was evaluated. In order to carry out an assessment on a national level, a detailed characterization and classification of the Norwegian islands was presented. Moreover, a multiple-step sorting procedure was implemented to identify 138 suitable installation sites and select 10 reference islands. A methodology was developed to estimate the electrical load and RES production and thus capture the specificities of the Norwegian sites. For the selected reference islands, the techno-economic optimization of the RES-P2P system was performed by adopting an optimization tool to determine the optimal system configuration that minimizes the LCOE while ensuring a reliable power supply service.

The most cost-effective configuration of RES-based energy systems involves the hybridization of renewable electricity production (PV and wind turbines) and storage (hydrogen and batteries). The resulting LCOE is in the range of 0.21 to 0.63 €/kWh. Specifically, it is around 0.2 €/kWh when the wind farm CF is above 50% and increases up to 0.6 €/kWh when the CF is close to 20%. The hybrid storage solution effectively combines the short-term capacity of high-efficiency batteries with the long-term capacity of hydrogen, which is able to cope with seasonal fluctuations in electrical load and RES production throughout the year. The hydrogen-based P2P prevents oversizing of the PV-wind system and minimizes the battery capacity that needs to be installed. Therefore, hydrogen is crucial to reduce the cost of electricity production when aiming for a 100% RES-based energy system.

The alternative electrification via submarine cables (0.14–1.47 €/kWh) involves high upfront costs for cable connection and its profitability depends heavily on the cable length and the annual electrical load of the island. For small islands (electricity demand close to 500 MWh/year), the cable scenario becomes economically favourable when the cable length is less than 5–15 km. The length below which the cable scenario is the cheapest solution increases with the amount of electrical load to be covered. Moreover, relying on fossil fuels was found to be economically unfeasible (0.87–1.04 €/kWh), mainly because of the high fuel price, which leads to significant operating costs.

In summary, the feasibility of RES-P2P systems in insular microgrid environments in Northern Europe can be assessed using the correlations derived in this study. In particular, the LCOE can be estimated and then compared to the cable-based configuration based on readily available data, i.e., RES capacity factor, distance from the mainland and annual energy consumption. This would help decision-makers to easily identify the most favourable solution for island power supply.

Based on the methodology here developed, future studies will explore the potential benefits arising from the hybridization of the scenarios discussed in this work, for example by integrating the RES-based solution with diesel generators and/or sea cable.

Acronyms and abbreviations

AT	Annual throughput
BT	Battery
CF	Capacity factor
CT	Curtailed
DG	Diesel generator
EES	Electrical energy storage
EL	Electrolyzer
EMS	Energy management strategy
FC	Fuel cell
HT	Hydrogen tank
LCOE	Levelized cost of electricity
LHV	Lower heating value
LPSP	Loss of power supply probability
LT	Lifetime throughput
NPC	Net present cost
O&M	Operation and maintenance
P2P	Power-to-Power
PEM	Proton exchange membrane
PSO	Particle swarm optimization
PV	Photovoltaic
PVGIS	Photovoltaic geographical information system
RES	Renewable energy sources
SC	Submarine cable
SOC	State of charge
STC	Standard test conditions
T&D	Transmission and distribution
TMY	Typical meteorological year
WT	Wind turbine

CRediT authorship contribution statement

Davide Trapani: Conceptualization, Methodology, Software, Validation, Formal analysis, Investigation, Resources, Data curation, Writing – original draft, Visualization. **Paolo Marocco:** Conceptualization, Methodology, Software, Investigation, Data curation, Writing – original draft, Writing – review & editing, Supervision. **Domenico Ferrero:** Writing – review & editing, Supervision. **Karen Byskov Lindberg:** Resources, Writing – review & editing. **Kyrre Sundseth:** Writing – review & editing, Supervision. **Massimo Santarelli:** Writing – review & editing, Supervision, Project administration, Funding acquisition.

Declaration of competing interest

The authors declare that they have no known competing financial interests or personal relationships that could have appeared to influence the work reported in this paper.

Data availability

Data will be made available on request.

Acknowledgements

This project has received funding from the Fuel Cells and Hydrogen 2 Joint Undertaking under grant agreement No 779541. This Joint Undertaking receives support from the European Union's Horizon 2020 research and innovation program, Hydrogen Europe and Hydrogen Europe research.

This publication is part of the project NODES which has received funding from the MUR – M4C2 1.5 of PNRR funded by the European Union - NextGenerationEU (Grant agreement no. ECS00000036).

References

[1] L. Xing, J. Wang, M. Dooner, J. Clarke, Overview of current development in electrical energy storage technologies and the application potential in power system operation, Appl. Energy 137 (2015) 511–536.
[2] IRENA, Battery Storage for Renewables: Market Status and Technology Outlook, International Renewable Energy Agency (IRENA), Abu Dhabi, 2015.
[3] IRENA, Electricity Storage and Renewables for Island Power A Guide for Decision Makers, International Renewable Energy Agency (IRENA), Abu Dhabi, 2012.
[4] Y. Kalinci, A. Hepbasli, I. Dincer, Techno-economic analysis of a stand-alone hybrid renewable energy system with hydrogen production and storage options, Int. J. Hydrog. Energy 40 (24) (2015) 7652–7664.
[5] O.V. Marchenko, S.V. Solomin, Modeling of hydrogen and electrical energy storages in wind/PV energy system on the Lake Baikal coast, Int. J. Hydrog. Energy 42 (15) (2017) 9361–9370.
[6] IRENA, Hydrogen From Renewable Power Technology Outlook for the Energy Transition, International Renewable Energy Agency (IRENA), Abu Dhabi, 2018.
[7] M. Gandiglio, P. Marocco, I. Bianco, D. Lovera, G.A. Blengini, M. Santarelli, Life cycle assessment of a renewable energy system with hydrogen-battery storage for a remote off-grid community, Int. J. Hydrog. Energy 47 (77) (2022) 32822–32834.
[8] D. Chade, T. Miklis, D. Dvorak, Feasibility study of wind- to-hydrogen system for Arctic remote locations–Grimsey island case study, Renew. Energy 76 (2015) 204–211.
[9] IRENA, Off-grid Renewable Energy Systems: Status and Methodological Issues, International Renewable Energy Agency, Abu Dhabi, 2015.
[10] J.M. Weinand, M. Hoffmann, J. Göpfert, T. Terlouw, J. Schönau, P. Kuckertz, R. McKenna, L. Kotzur, J. Linßen, D. Stolten, Global LCOEs of decentralized off-grid renewable energy systems, Renew. Sust. Energ. Rev. 183 (113478) (2023).
[11] Z. Chmiel, S.C. Bhattacharyya, Analysis of off-grid electricity system at isle of Eigg (Scotland): lessons for developing countries, Renew. Energy 81 (2015) 578–588.
[12] L.K. Gan, J.K. Shek, M.A. Mueller, Hybrid wind– photovoltaic–diesel–battery system sizing tool development using empirical approach, life-cycle cost and performance analysis: a case study in Scotland, Energy Convers. Manag. 106 (2015) 479–494.
[13] D. Roy, Modelling an off-grid hybrid renewable energy system to deliver electricity to a remote Indian Island, Energy Convers. Manag. 281 (116839) (2023).
[14] J. Kaldellis, D. Zafirakis, Optimum sizing of stand-alone wind-photovoltaic hybrid systems for representative wind and solar potential cases of the Greek territory, J. Wind Eng. Ind. Aerodyn. 107 (2012) 169–178.
[15] T. Ma, H. Yang, L. Lu, A feasibility study of a stand-alone hybrid solar–wind–battery system for a remote island, Appl. Energy 121 (2014) 149–158.
[16] X. Qi, J. Wang, G. Królczyk, P. Gardoni, Z. Li, Sustainability analysis of a hybrid renewable power system with battery storage for islands application, J. Energy Storage 50 (104682) (2022).
[17] P. Enevoldsen, B.K. Sovacool, Integrating power systems for remote island energy supply: lessons from Mykines, Faroe Islands, Renew. Energy 85 (2016) 642–648.
[18] O.S. Parissis, E. Zoulias, E. Stamatakis, K. Sioulas, L. Alves, R. Martins, A. Tsikalakis, N. Hatziargyriou, G. Caralis, A. Zervos, Integration of wind and hydrogen technologies in the power system of Corvo island, Azores: a cost-benefit analysis, Int. J. Hydrog. Energy 36 (13) (2011) 8143–8151.
[19] G. Tzamalis, E.I. Zoulias, E. Stamatakis, O.S. Parissis, A. Stubos, E. Lois, Techno-economic analysis of RES & hydrogen technologies integration in remote island power system, Int. J. Hydrog. Energy 38 (26) (2013) 11646–11654.
[20] D.R. Fragoso, A. dos Santos, E.C. Fernandes, Increasing RES penetration through H2 technologies on Flores island, Azores: a techno-economic analysis, Int. J. Hydrog. Energy 48 (52) (2023) 19846–19861.

[21] P. Marocco, D. Ferrero, A. Lanzini, M. Santarelli, Optimal design of stand-alone solutions based on RES+ hydrogen storage feeding off-grid communities, Energy Convers. Manag. 238 (2021).
[22] W. Dong, Y. Li, J. Xiang, Optimal sizing of a stand-alone hybrid power system based on battery/hydrogen with an improved ant colony optimization, Energies 9 (10) (2016).
[23] X. Zhang, Q.S. Wei, B.S. Oh, Cost analysis of off-grid renewable hybrid power generation system on Ui Island, South Korea, Int. J. Hydrog. Energy 47 (27) (2022) 13199–13212.
[24] P. Marocco, R. Novo, A. Lanzini, G. Mattiazzo, M. Santarelli, Towards 100% renewable energy systems: the role of hydrogen and batteries, J. Energy Storage 57 (106306) (2023).
[25] D. Groppi, D. Astiaso Garcia, G. Lo Basso, F. Cumo, L. De Santoli, Analysing economic and environmental sustainability related to the use of battery and hydrogen energy storages for increasing the energy independence of small islands, Energy Convers. Manag. 177 (2018) 64–76.
[26] J. Tariq, Energy management using storage to facilitate high shares of variable renewable energy, Int. J. Sustain. Energy Plan. Manag. 25 (2020) 61–76.
[27] REMOTE Project Official Website [Online]. Available: https://www.remote-euproject.eu/, 2018 [Accessed March 2023].
[28] P. Marocco, D. Ferrero, M. Gandiglio, M. Ortiz, K. Sundseth, A. Lanzini, M. Santarelli, A study of the techno-economic feasibility of H2-based energy storage systems in remote areas, Energy Convers. Manag. 211 (2020).
[29] P. Marocco, D. Ferrero, A. Lanzini, M. Santarelli, The role of hydrogen in the optimal design of off-grid hybrid renewable energy systems, J. Energy Storage 46 (2022).
[30] Ø. Ulleberg, T. Nakken, A. Ete, The wind/hydrogen demonstration system at Utsira in Norway: evaluation of system performance using operational data and updated hydrogen energy system modelling tools, Int. J. Hydrog. Energy 35 (5) (2010) 1841–1852.
[31] K. Solbakken, B. Babar, T. Boström, Correlation of wind and solar power in high-latitude arctic areas in Northern Norway and Svalbard, Renew. Energy Environ. Sustain. 1 (42) (2016).
[32] "Store Norske Leksikon," Store Norske Leksikon, [Online]. Available: https://snl.no/. [Accessed March 2023].
[33] NVE Atlas, Norwegian Water Resources and Energy Directorate [Online]. Available: https://atlas.nve.no/Html5Viewer/index.html?viewer=nveatlas# [Accessed March 2023].
[34] A. Kipping, E. Trømborg, Modeling and disaggregating hourly electricity consumption in Norwegian dwellings based on smart meter data, Energ. Buildings 118 (2016) 350–369.
[35] V. Bøe, Cost Optimization of Distributed Power Generation in Southern Norway, with Focus on Renewable Hybrid System Configurations, Norwegian University of Life Sciences, Ås, 2017.
[36] S. Shiplu, Feasibility analysis of a renewable hybrid energy system with producer gas generator fulfilling remote household electricity demand in Southern Norway, Renew. Energy 87 (2016) 772–781.
[37] HOMER Pro User Manual [Online]. Available: https://www.homerenergy.com/products/pro/docs/3.13/index.html [Accessed September 2023].
[38] K.B. Lindberg, S.J. Bakker, I. Sartori, Modelling electric and heat load profiles of non-residential buildings for use in long-term aggregate load forecasts, Util. Policy 58 (2019) 63–88.
[39] I. Sartori, B.J. Wachenfeldt, A.G. Hestnes, Energy demand in the Norwegian building stock: scenarios on potential reduction, Energy Policy 37 (5) (2009) 1614–1627.
[40] O. Stavset, H. Kauko, Energy Use in Non-residential Buildings-Possibilities for Smart Energy Solutions, SINTEF, 2015.
[41] Statistics Norway, Energy Use, by Energy Product, Type of Building, Contents and Year [Online]. Available: https://www.ssb.no/en/statbank/table/09743/ [Accessed March 2023].
[42] Photovoltaic Geographical Information System (PVGIS) [Online]. Available: https://ec.europa.eu/jrc/en/pvgis [Accessed March 2023].
[43] C. Ghenai, T. Salameh, A. Merabet, Technico-economic analysis of off grid solar PV/fuel cell energy system for residential community in desert region, Int. J. Hydrog. Energy 45 (20) (2020) 11460–11470.
[44] J.A. Duffie, W.A. Beckman, N. Blair, Solar Engineering of Thermal Processes, Photovoltaics and Wind, John Wiley & Sons, 2020.
[45] M.R. Quitoras, P.E. Campana, C. Crawford, Exploring electricity generation alternatives for Canadian Arctic communities using a multi-objective genetic algorithm approach, Energy Convers. Manag. 210 (2020).
[46] LG, LG NeON® R Solar Module [Online]. Available: https://www.lg.com/us/business/solar-panels/lg-LG365Q1C-A5 [Accessed March 2023].
[47] Wind Energy Solutions WES [Online]. Available: https://windenergysolutions.nl/, 2021 [Accessed March 2023].
[48] P. Rullo, L. Braccia, P. Luppi, D. Zumoffen, D. Feroldi, Integration of sizing and energy management based on economic predictive control for standalone hybrid renewable energy systems, Renew. Energy 140 (2019) 436–451.
[49] L. Gracia, P. Casero, C. Bourasseau, Use of hydrogen in off-grid locations, a techno-economic assessment, Energies 11 (11) (2018) 3141.
[50] L. Moretti, M. Astolfi, C. Vergara, E. Macchi, J. Pérez-Arriaga, G. Manzolini, A design and dispatch optimization algorithm based on mixed integer linear programming for rural electrification, Appl. Energy 233 (2019) 1104–1121.
[51] B.K. Das, M. Hasan, P. Das, Impact of storage technologies, temporal resolution, and PV tracking on stand-alone hybrid renewable energy for an Australian remote area application, Renew. Energy 173 (2021) 362–380.
[52] M. Sharafi, T. El Mekkawy, Multi-objective optimal design of hybrid renewable energy systems using PSO-simulation based approach, Renew. Energy 68 (2014) 67–69.
[53] N. Destro, A. Benato, A. Stoppato, A. Mirandola, Components design and daily operation optimization of a hybrid system with energy storages, Energy 117 (2016) 569–577.
[54] T. Tezer, R. Yaman, G. Yaman, Evaluation of approaches used for optimization of stand-alone hybrid renewable energy systems, Renew. Sust. Energ. Rev. 73 (2017) 840–853.
[55] A. Maleki, A. Askarzadeh, Comparative study of artificial intelligence techniques for sizing of a hydrogen-based stand-alone photovoltaic/wind hybrid system, Int. J. Hydrog. Energy 39 (19) (2014) 9973–9984.
[56] M. Boussetta, R. El Bachtiri, M. Khanfara, K. El Hammoumi, Assessing the potential of hybrid PV–wind systems to cover public facilities loads under different Moroccan climate conditions, Sustain. Energy Technol. Assess. 22 (2017) 74–82.
[57] Federal Ministry for Economic Affairs and Energy, Markets for Battery Storage. Sub-sector Analysis on the Market Potential for Battery Storage in Tanzania, 2015.
[58] J. Proost, State-of-the art CAPEX data for water electrolysers, and their impact on renewable hydrogen price settings, Int. J. Hydrog. Energy 44 (9) (2019) 4406–4413.
[59] M. Shehzad, M. Abdelghany, D. Liuzza, V. Mariani, L. Glielmo, Mixed logic dynamic models for MPC control of wind farm hydrogen-based storage systems, Inventions 4 (4) (2019).
[60] Tractebel, Hinicio, Study on Early Business Cases for H2 in Energy Storage and More Broadly Power to H2 Applications [Online]. Available: https://www.fch.europa.eu/sites/default/files/P2H_Full_Study_FCHJU.pdf, 2017.
[61] M. Santos, I. Marino, Energy Analysis of the Raggovidda Integrated System [Online]. Available: https://www.haeolus.eu/wp-content/uploads/2019/01/D5.1.pdf, 2019.
[62] Battelle Memorial Institute, Manufacturing Cost Analysis of PEM Fuel Cell Systems for 5- and 10-kW Backup Power Applications [Online]. Available: https://energy.gov/sites/prod/files/2016/12/f34/fcto_cost_analysis_pem_fc_5-10kw_backup_power_0.pdf, 2016.
[63] B. Li, R. Roche, A. Miraoui, Microgrid sizing with combined evolutionary algorithm and MILP unit commitment, Appl. Energy 188 (2017) 547–562.
[64] J. Torreglosa, P. García-Triviño, L. Fernández-Ramirez, F. Jurado, Control based on techno-economic optimization of renewable hybrid energy system for stand-alone applications, Expert Syst. Appl. 51 (2016) 59–75.
[65] TrønderEnergi [Online]. Available: https://tronderenergi.no/ [Accessed September 2023].
[66] E.A. Bergmann, New Electric Power Supply of the Island of Myken on Helgelandskysten, Norwegian University of Life Sciences, 2014.
[67] Oslo Economics, Kabel som alternativ til luftledning, 2022.
[68] A. Malheiro, P. Castro, R. Lima, A. Estanqueiro, Integrated sizing and scheduling of wind/PV/diesel/battery isolated systems, Renew. Energy 83 (2015) 646–657.
[69] A.Q. Jakhrani, A.R.H. Rigit, A.K. Othman, S.R. Samo, S.A. Kamboh, Estimation of carbon footprints from diesel generator emissions, in: International Conference on Green and Ubiquitous Technology, 2012, pp. 78–81.
[70] D. Bionaz, P. Marocco, D. Ferrero, K. Sundseth, M. Santarelli, Life cycle environmental analysis of a hydrogen-based energy storage system for remote applications, Energy Rep. 8 (2022) 5080–5092.
[71] G. Prevedello, A. Werth, The benefits of sharing in off-grid microgrids: a case study in the Philippines, Appl. Energy 303 (2021).